Original Article

MOLECULAR METABOLISM

Whole body and hematopoietic cell-specific deletion of G-protein coupled receptor 65 (GPR65) improves insulin sensitivity in diet-induced obese mice

Yingjiang Zhou[1], EunJu Bae[2], Simon S. Hoffman[1], Da Young Oh[3], Gordon I. Smith[4], Samuel Klein[4], Saswata Talukdar[1,*]

ABSTRACT

Objective: Acidic extracellular microenvironments, resulting from enhanced glycolysis and lactic acid secretion by immune cells, along with metabolic acidosis may interfere with the insulin signaling pathway and contribute to the development of insulin resistance. In the present study, we investigated the role of G protein-coupled receptor GPR65, an extracellular pH sensing protein, in modulating insulin resistance.

Methods: We measured *GPR65* expression in the adipose tissue (AT) of subjects with varying metabolic health states. We utilized whole-body and hematopoietic cell-specific GPR65 knockout (KO) mice to investigate the mechanism underlying the associations between GPR65, inflammatory response, and insulin resistance.

Results: Elevated *GPR65* expression was observed in the AT of subjects with obesity, compared to their lean counterparts, and was inversely correlated with insulin resistance. In GPR65 KO mice, improved insulin sensitivity and decreased hepatic lipid content were observed, attributed to concomitant increases in mitochondrial activity and fatty acid β-oxidation in liver. GPR65 KO mice also exhibited increased Akt phosphorylation in skeletal muscle, suppressed proinflammatory gene expression in AT, and decreased serum cytokine levels, collectively suggesting the anti-inflammatory effects of GPR65 depletion. This was further confirmed by observations of decreased macrophage chemotaxis towards AT *in vitro*, and depressed inflammatory signaling pathway activation in bone marrow-derived dendritic cells from GPR65 KO mice. Additionally, hematopoietic lineage-specific GPR65 KO mice exhibited improved whole body insulin sensitivity in clamp studies, demonstrating GPR65 signaling in immune cells mediates this effect.

Conclusions: Our data suggests that macrophage-specific GPR65 signaling contributes to inflammation and the development of insulin resistance.

Keywords GPR65; Inflammation; Insulin resistance; Obesity; Hyperinsulinemic-euglycemic clamp

1. INTRODUCTION

Insulin resistance is a hallmark of the metabolically unhealthy obese population and is an initiating event in the development of type 2 diabetes (T2D) and associated metabolic sequalae [1]. Several studies have established chronic, low-grade inflammation as a key contributor to the etiology of insulin resistance [2—4]. In adipose tissue (AT), inflammation is often instigated by rapid adipocyte hypertrophy in response to overnutrition, which pushes lipid-laden adipocytes outside the oxygen diffusion gradient of existing capillaries, resulting in localized hypoxia and cell death [4]. Resultant cellular debris then promotes immune cell infiltration and incites resident AT macrophages (ATMs) to polarize towards a pro-inflammatory or "M1" like phenotype, leading to pro-inflammatory cytokine production [5]. Thereafter, activated inflammatory signaling pathways impair both local and systemic insulin signaling [6,7].

Importantly, insulin sensitivity in other tissues such as skeletal muscle and liver are also influenced by local immune cell activity, where resident and recruited macrophage populations similarly polarize to a pro-inflammatory phenotype during the development of obesity [8]. Inflammation exerts effects on the extracellular microenvironment beyond cytokine release, demonstrated by inflammatory responses in peripheral tissues predisposing the development of acidic microenvironments [9]. The acidic microenvironment of inflammatory loci is partly attributed to increased lactate production by the anaerobic glycolysis of infiltrated neutrophils [10,11]. However, increased extravasation of fluid into local tissue from inflammation increases the oxygen diffusion distance to cells and infiltration of circulating immune

[1]Merck & Co., Inc., South San Francisco, CA, USA [2]Jeonbuk National University, Jeonju, South Korea [3]UT Southwestern Medical Center, Dallas, TX, USA [4]Center for Human Nutrition, Washington University, St. Louis, MO, USA

*Corresponding author. Merck & Co., Inc., 213 East Grand Ave, South San Francisco, CA, 94080, USA. E-mail: Saswata.Talukdar@merck.com (S. Talukdar).

Received April 8, 2025 • Revision received May 9, 2025 • Accepted May 14, 2025 • Available online 17 May 2025

https://doi.org/10.1016/j.molmet.2025.102169

cells further depletes available oxygen, rendering resident cells hypoxic. This, in turn, drives metabolic adaptations in fuel utilization favoring anaerobic glycolysis and producing lactate, which is exported from the cell through a proton-coupled process, further decreasing local pH [12]. In line with these observations, obese mice with adipocyte-selective knockdown of lactate dehydrogenase A have reduced inflammatory ATM accumulation and are protected from obesity-associated glucose intolerance and insulin resistance. Moreover, human adipose tissue lactate levels are positively correlated with both inflammatory gene expression and insulin resistance independent of body mass index (BMI) [13]. People with obesity and diabetes have been shown to have lower blood pH [14], and local low pH has been shown to inhibit insulin signaling in several tissues [8]. Moreover, metabolic acidosis induced in lean insulin-sensitive individuals results in impaired insulin signaling, suggesting this effect is not dependent on obesity or impaired metabolic function *per se* [15]. Thus, it is important to investigate how immune cells are influenced by the acidic microenvironments commonly found in tissues with excess fat accumulation, as this may affect immune cell function, cytokine production, and the initiation or worsening of insulin resistance.

One potential regulator of immune cell function in an acidic microenvironment is G protein-coupled receptor GPR65 (*aka* T cell death-associated gene 8/TDAG8) which is an extracellular pH sensor primarily expressed in lymphoid tissues [16]. Previous studies have demonstrated that GPR65 senses extracellular pH or proton concentration via their histidine residues, stimulating adenylyl cyclase activity and the subsequent accumulation of intracellular cyclic AMP (cAMP) [17]. However, the pathophysiological function of GPR65 in the context of obesity and insulin resistance is incompletely understood. *GPR65* is highly expressed in the immune system of humans, implying a potential immunometabolic role in metabolic disorders where the incidence of acidosis is high [18]. Indeed, *GPR65* has been shown to be a susceptibility gene for inflammatory bowel disease (IBD), where it regulates gut inflammation by promoting the differentiation of $CD4^+$ Th1 and Th17 cells [19]. Interestingly, the role of GPR65 as a metabolic regulator may extend beyond pH sensing in immune cells as it is expressed on a subpopulation of vagal afferent neurons innervating intestinal villi [20] which act as nutrient sensors and may regulate hepatic glucose production [21].

Although tissue acidosis and inflammation both contribute to insulin resistance and are mediated by immune cell activity, the role of GPR65 in obesity-driven metabolic diseases remains unknown. We made the novel observation that *GPR65* expression in the AT of humans is increased with metabolically unhealthy obesity, suggesting GPR65 may play a role in modulating metabolism in other metabolically active tissues. Thus, we sought to examine the role of GPR65 in multi-organ immune cell-mediated insulin resistance. To this end, we fed GPR65 knockout (KO) animals a high-fat diet and interrogated the effects of GPR65 deficiency on glucose disposal, tissue insulin sensitivity, and inflammation. In addition, we make key correlations between immune cell *GPR65* expression and inflammatory signaling pathway activation, chemotaxis, and immune cell polarization. Together, we demonstrate that GPR65 regulates the acidosis-induced proinflammatory response of macrophages and modulates tissue inflammation and insulin resistance in metabolic disorders.

2. METHODS

2.1. Clinical study

A total of 53 subjects (12 men and 41 women) participated in this study. The results represent a new analysis of adipose tissue samples and data that were obtained during the participants' involvement in another study that evaluated the metabolic heterogeneity among people who are lean or with obesity [22]. Three groups were studied: 1) metabolically-healthy lean (MHL, $n = 15$) defined as a body mass index (BMI) of 18.5–24.9 kg/m^2, with normal fasting plasma glucose (<100 mg/dL), oral glucose tolerance (2-h oral glucose tolerance test (OGTT) plasma glucose <140 mg/dL) and intrahepatic triglyceride content (IHTC) (≤5% of liver volume as triglyceride); metabolically-healthy obese (MHO, $n = 19$) defined as a BMI of 30.0–49.9 kg/m^2 with normal fasting plasma glucose, oral glucose tolerance and IHTC; and 3) metabolically-unhealthy obese (MUO, $n = 19$) defined as a BMI of 30.0–49.9 kg/m^2, with impaired fasting glucose (100–125 mg/dL) or impaired oral glucose tolerance (2-h OGTT plasma glucose 140–199 mg/dL) and high IHTC (≥6%). The study was conducted in the Clinical Translational Research Unit (CTRU) at Washington University School of Medicine in St. Louis, MO. Participants provided written, informed consent before participating in this study, which was approved by the Institutional Review Board at Washington University School of Medicine in St. Louis, MO, and registered at ClinicalTrials.gov (NCT02706262). Potential participants who had a history of diabetes or liver disease other than metabolic dysfunction-associated steatotic liver disease (MASLD), were taking medications that can affect glucose or lipid metabolism, consumed excessive amounts of alcohol (>21 units of alcohol per week for men and >14 units of alcohol per week for women), or were pregnant or lactating were excluded.

Details of the research methods have been described previously [22]. Total body fat and fat-free mass (FFM) were determined by using dual-energy x-ray absorptiometry and IHTC was determined by using magnetic resonance imaging. Serial 24-hour (hourly from 7:00 am to 11:00 pm and from 5:00 am to 7:00 am) plasma glucose and insulin concentrations were obtained to assess 24-hour plasma glucose and insulin concentration areas-under-the curve (AUC). Skeletal muscle insulin sensitivity, assessed by using the hyperinsulinemic-euglycemic clamp procedure (insulin infusion rate of 50 mU/m^2 body surface area/min), in conjunction with stable isotopically labeled glucose tracer infusion, was calculated as glucose rate of disposal (Rd) expressed per kg FFM divided by the average plasma insulin concentration (glucose R_d/Insulin) during the final 20 min of the clamp procedure [23]. Hepatic insulin sensitivity was assessed by using the Hepatic Insulin Sensitivity Index calculated as the inverse of the product of plasma insulin concentration and the endogenous glucose rate of appearance into the systemic circulation, determined by dividing the glucose tracer infusion rate by the average plasma glucose tracer-to-tracee ratio during the last 20 min of the basal period of the clamp procedure [24]. Periumbilical subcutaneous abdominal adipose tissue was obtained by percutaneous liposuction during the basal period of the clamp procedure, flash frozen in liquid nitrogen and stored at −80 °C until processing for RNA sequencing.

2.2. Chemicals and reagents

All chemicals and reagents were purchased from Sigma–Aldrich unless stated otherwise.

2.3. Animal care and use

Male C57BL/6 mice or homozygous GPR65 KO and WT littermates were acquired from Taconic Biosciences (Germantown, NY) at 8 weeks of age and housed on a 12 h light/dark cycle with ad libitum access to water and a 60% high-fat diet (HFD; D12492, Research Diets) for 16–20 weeks. All procedures detailed here were approved by the Institutional Animal Care and Use Committee.

2.4. Adipose tissue macrophages (ATMs) isolation and fluorescence-activated cell sorting (FACS) analysis of ATMs

ATM isolation from adipose tissue stromal vascular cells (SVCs) and FACS analysis were performed as previously described [25]. Briefly, epididymal fat pads were weighed, rinsed three times in PBS, and then minced in FACS buffer (PBS + 1% low endotoxin BSA). Tissue suspensions were treated with collagenase (1 mg/mL, Sigma—Aldrich) for 30 min, and then filtered through a 100 μm filter (BD Biosciences). After centrifugation at 500 *g* for 5 min, the supernatant containing adipocytes was removed and the pellet containing the SVC fraction was incubated in RBC lysis buffer (eBioscience) for 5 min followed by another centrifugation (300 *g*, 5 min) and resuspension in FACS buffer. SVCs were incubated with Fc Block (BD Biosciences) for 20 min at 4 °C before staining with fluorescently labeled primary antibodies or control IgGs for 30 min at 4 °C. F4/80-APC FACS antibody was purchased from AbD Serotec (Raleigh, NC); FITC-CD11b and PE-CD11c FACS antibodies were from BD Biosciences. Cells were gently washed twice and resuspended in FACS buffer with propidium iodide (Sigma—Aldrich). SVCs were analyzed using a FACSAria flow cytometer (BD Biosciences). Unstained, single stains and Fluorescence Minus One controls were used for setting compensation and gates. The events were first gated based on Forward-area *versus* Side scatter-area as well as Side scatter-height *versus* Side scatter-width and Forward scatter-height *versus* Forward scatter-width for a total of three dual parameter plots to gate out aggregates and debris. Single color controls were used to calculate compensation using the FACSDiva software. A plot of Forward scatter *versus* propidium iodide was used as the fourth gate to identify individual, live cells. To measure markers with the maximum sensitivity, each fluorochrome was plotted *versus* propidium iodide, and polygons were drawn, angled with the aid of the Fluorescence Minus One controls.

2.5. Mouse metabolic studies

Hyperinsulinemic-euglycemic clamp studies were performed as previously described [26]. Briefly, mice underwent surgical dual catheterization of the right jugular vein. Catheters were tunneled subcutaneously and exteriorized in the intrascapular region, allowing for free rein of movement during the clamp procedure. Mice which exhibited >4% loss of their pre-cannulation body weight after 4—5 days of recovery were excluded from the study. On the day of clamp mice were fasted for 6 h and baseline blood glucose measured via tail nick at −10 and 0 min using a handheld glucometer (AlphaTRAK2, Abbot Laboratories). While restrained, mice received a constant jugular infusion of D-[3-^{3}H] glucose (5 μCi/h; DuPont-NEN) for 90 min during equilibration, then an infusion of glucose (50% dextrose, variable infusion rate; Abbott), tracer (5 μCi/h), and insulin (6 mU/kg/min). Serial blood sampling was performed every 10 min via tail vein nick for blood glucose monitoring, and plasma glucose measurements reached steady state conditions (120 ± 10 mg/dL) for a minimum of 30 min by the end of the procedure. Tracer-determined rates were calculated using the Steele equation as previously described [27].

For oral glucose tolerance tests (OGTT) mice were fasted for 7 h, baseline blood drawn via tail vein nick, and then an intraperitoneal (i.p.) dose of 1 g/kg^{-1} dextrose administered as previously described [28]. Serial blood draws were then taken via tail vein nick at indicated timepoints and assayed via a handheld glucometer (AlphaTRAK2, Abbot Laboratories).

2.6. Biochemical analysis

Total RNA was isolated from flash frozen tissue samples using Qiazol reagent (Qiagen) and RNeasy columns (Qiagen) according to manufacturer's instructions. RNA purity and quality was analyzed via nanodrop spectrophotometry (ThermoFisher). First-strand cDNA was synthesized using a High-Capacity cDNA Reverse Transcription Kit (Applied Biosystems). Quantitative PCR (qPCR) was run as a 20 μL reaction using a MJ Research PTC-200 96-well thermocycler coupled with the Chromo 4 Four-Color Real-Time System (GMI Inc.). Gene expression was calculated using the $\Delta\Delta C_T$ method normalized to the housekeeping gene *GAPDH* then expressed as relative mRNA values compared to internal control. RNA sequencing of human AT samples was performed as previously described [22].

Western blots were run using cell or tissue lysates extracted with RIPA buffer supplemented with a protease inhibitor cocktail (HALT, ThermoFisher). 20 μg of protein was separated using pre-cast SDS gels composed of 10% polyacrylamide (Bio-Rad), then transferred onto a polyvinylidene difluoride membrane (Immobilon, Milipore). Western blots were then stained and imaged as previously described [29]. All antibodies detailed here were acquired from Cell Signaling Technology. Cellular ATP was analyzed via enzyme-linked immunosorbent assay (ELISA) (BioSource) on lysates prepared as above and normalized to total cellular protein via BCA assay (Pierce, ThermoFisher). NAD/NADH ratio was determined colorimetrically using a specific kit (Abcam). Mouse serum cytokines were assayed using an MSD multiplex kit (MesoScale Discovery) according to manufacturer's instructions.

2.7. Liver histology and lipid content measurement

Liver tissue was embedded in OCT then flashes frozen in liquid nitrogen and cryosectioned in 10 mm slices before being fixed for 20 min in PFA. Neutral lipids were stained via Oil red O and imaged. Liver triglycerides were extracted from frozen tissue using a 2:1 mixture of chloroform and methanol (Folch method) and assayed using Triglyceride-SL assay kit (Genzyme Diagnostics).

2.8. Palmitic acid oxidation assay

For the palmitic acid oxidation assay liver homogenates (~40 μL) were pre-incubated for 15 min at 30 °C as previously described [30]. Homogenates were then combined with 160ul of oxidation buffer (described elsewhere [31]), followed by [1−^{14}C]Palmitate (0.5 μCi/mL, final concentration) in an albumin complex (molar ratio of 5:1). Reactions were allowed to progress for 60 min before being halted by the addition of 200 μL of 3 M $HClO_4$, followed by an additional incubation step for 75 min at 4 °C. An organic solvent mixture composed of ethanolamine and ethylene glycol (300 μL; 1:1, *v/v*) was used to trap the released radiolabeled CO_2. The mixture was then centrifuged at 10,000 *g* for 1 min and supernatant radioactivity assayed via liquid scintillation counting. Palmitate oxidation rates were calculated as described by Glatz et al. [32] from the sum of $^{14}CO_2$ and ^{12}C-labeled acid-soluble products.

2.9. Cell culture

3T3-L1 adipocytes were acquired from American Type Culture Collection (ATCC) and grown and passaged in high-glucose Dulbecco's modified Eagle's medium DMEM (Hyclone) containing 4500 mg/L glucose and 4 mM L-Glutamine and supplemented with 10% (*v/v*) low endotoxin fetal bovine serum (FBS; Gibco) and 1% (*v/v*) penicillin-streptomycin (Gibco) (basic media) and maintained in a humidified incubator at 37 °C and 5% CO_2. Cells were grown to confluence, then 2 days post confluency (day 0) differentiation was initiated via supplementation of the same media with 3 isobutyl-1-methylxanthine (IBMX; 500 μM), dexamethasone (25 μM), and insulin (4 μg/mL) for 2 days. Media was replaced with basic media containing 4 μg/mL insulin on days 2, 5, and 8, and then with basic media alone on day 11

for conditioned media harvesting on day 12. The collected media was aliquoted and frozen at −20 °C until the time of chemotaxis assay.
Bone marrow cells were acquired from flushing the tibial and femoral medullary cavities of GPR65 KO mice or WT littermates with RPMI medium (Gibco). Cells were washed and seeded into tissue culture plates and maintained in RPMI media supplemented with 20% low endotoxin FBS and 1% penicillin-streptomycin. Cells underwent directed differentiation towards bone marrow-derived macrophages (BMDMs) or bone marrow-derived dendritic cells (BMDCs) via supplementation with L-929 conditioned medium (30%, *v/v*) or recombinant GM-CSF (40 ng/mL), respectively. Differentiation was complete 8 days post-plating when expression of F4/80 and CD11c have been demonstrated to be high [33].

2.10. *In vitro* chemotaxis assay

Chemotaxis assays and intraperitoneal macrophage isolation were performed as previously described [34]. Fully differentiated 3T3-L1 adipocytes were used for preparation of conditioned media and harvested solely from adipocytes demonstrating large lipid droplets 12 days after differentiation. For the migration assay, intraperitoneal macrophages were isolated from GPR65 KO mice or WT littermates via thioglycollate challenge. Briefly, 1 mL of 3.8% brewers thioglycollate medium was injected into the animals' abdominal cavity to incite macrophage accumulation. After 3 days mice were euthanized under isoflurane anesthesia and 3 mL of ice-cold DPBS were injected and massaged into the peritoneal cavity. The fluid was recovered, and intraperitoneal macrophages were pelleted via centrifugation before being resuspended in RPMI medium. Intraperitoneal macrophages (100,000 cells/condition) were placed in the upper chamber of an 8 mM polycarbonate filter (24-transwell format; Corning), with adipocyte conditioned medium placed in the lower chamber. Cells were allowed to migrate for a duration of 3 h before undergoing formalin fixation and staining with 4', 6-diamidino-2-phenylindole for counting.

2.11. Bone marrow transplantation

Bone marrow cells were obtained from male GPR65 KO mice or WT littermates then injected into irradiated at 1,000 rad 8-week-old male C57BL/6 mice via the tail vein ($\sim 3 \times 10^6$ cells/animal). Mice were maintained on an HFD for 16 weeks following injection. The reconstitution of donor marrow was confirmed after 4 weeks via qPCR.

2.12. Data analysis & statistics

Densitometric quantification and normalization were performed using ImageJ 1.42q software (NIH). Statistical analyses were conducted with Prism software version 9.4.1 (GraphPad, San Diego, CA). Comparisons between two groups were analyzed using Student's unpaired t-test. Comparisons between three or more groups were analyzed using one-way analysis of variance (ANOVA), with Bonferroni or Fisher's least significant difference post-hoc test used to locate significant mean differences when appropriate. Relationships between adipose tissue *GPR65* and hepatic and whole-body insulin sensitivity were evaluated using linear and nonlinear regression analysis with the best-fit to the data reported. Data is presented as means ± SEM. Statistical significance was defined as $P < 0.05$.

3. RESULTS

3.1. *GPR65* expression is elevated in the adipose tissue of people with obesity, and in the adipose tissue pro-inflammatory macrophage population of HFD-fed mice

We first sought to determine the relevance of adipose tissue (AT) *GPR65* expression on metabolic function in humans with different metabolic states. To achieve this, we conducted a hyperinsulinemic-euglycemic clamp in metabolically healthy lean (MHL) subjects, as well as those with metabolically healthy obesity (MHO) or metabolically unhealthy obesity (MUO) and correlated AT *GPR65* expression with hepatic and skeletal muscle insulin sensitivity.
Body composition and metabolic characteristics of the study participants are shown in Table 1. There were no differences in body mass index (BMI), percent body weight as fat, or fat-free mass (FFM) between MHO and MUO groups ($P > 0.05$; Table 1). However, IHTC, HbA1c, plasma glucose variables (fasting 2-hour OGTT and 24-hour plasma glucose AUC), and 24-hour plasma insulin AUC were greater and hepatic and skeletal muscle insulin sensitivity were lower in the MUO than the MHO group ($P < 0.05$; Table 1). Hepatic and skeletal muscle insulin sensitivity were greater in the MHL than the MHO group ($P < 0.05$; Table 1). Adipose tissue expression of *GPR65* progressively increased from the MHL to the MHO to the MUO groups ($P < 0.05$; Figure 1A) and was inversely correlated with skeletal muscle insulin sensitivity ($r = -0.68$, $P < 0.05$; Figure 1B) and hepatic insulin sensitivity ($r = -0.67$, $P < 0.05$; Figure 1C). Taken together, in

Table 1 — Body composition and metabolic characteristics of the participants.

	MHL ($n = 15$)	MHO ($n = 19$)	MUO ($n = 19$)
Age (yr)	36.0 ± 2.3	39.7 ± 1.8	39.4 ± 2.0
Body mass index (kg/m^2)	22.7 ± 0.4	38.9 ± 1.2[a]	39.4 ± 1.1[a]
Body mass (kg)	64.1 ± 1.8	109.0 ± 3.9[a]	109.9 ± 4.5[a]
Fat-free mass (kg)	45.6 ± 1.7	54.6 ± 2.0[a]	56.7 ± 2.3[a]
Body fat (%)	28 ± 2	49 ± 1[a]	48 ± 1[a]
Intrahepatic triglyceride content (%)	1.6 ± 0.1	2.5 ± 0.2	15.7 ± 1.7[ab]
HbA1c (%)	5.0 ± 0.1	5.1 ± 0.1	5.7 ± 0.2[ab]
Fasting glucose (mg/dL)	85 ± 1	88 ± 1	99 ± 2[ab]
OGTT 2-h plasma glucose (mg/dL)	97 ± 5	106 ± 4	169 ± 8[ab]
24-h glucose AUC (mg/dL x 24 h)	2,273 ± 43	2,295 ± 30	2,668 ± 40[ab]
24-h Insulin AUC (μU/mL x 24 h)	548 ± 77	1,087 ± 98	2,223 ± 302[ab]
Hepatic insulin sensitivity index [1,000/(μmol/kg FFM/min)*(μU/mL)]	11.3 ± 1.1	5.8 ± 0.5[a]	3.0 ± 0.2[ab]
Skeletal muscle insulin sensitivity [Glucose Rd (nmol/kg FFM/min)/Insulin (μU/mL)]	636 ± 42	421 ± 40[a]	192 ± 7[ab]

Data are expressed as mean ± SEM. FFM, fat-free mass. OGTT, Oral glucose tolerance test. Glucose Rd, glucose rate of disappearance. Two-tailed one-way ANOVAs and Bonferroni post-hoc procedure were used to identify significant differences between groups.
[a] $P \leq 0.05$ value significantly different from MHL value.
[b] $P \leq 0.05$ value significantly different from MHO value.

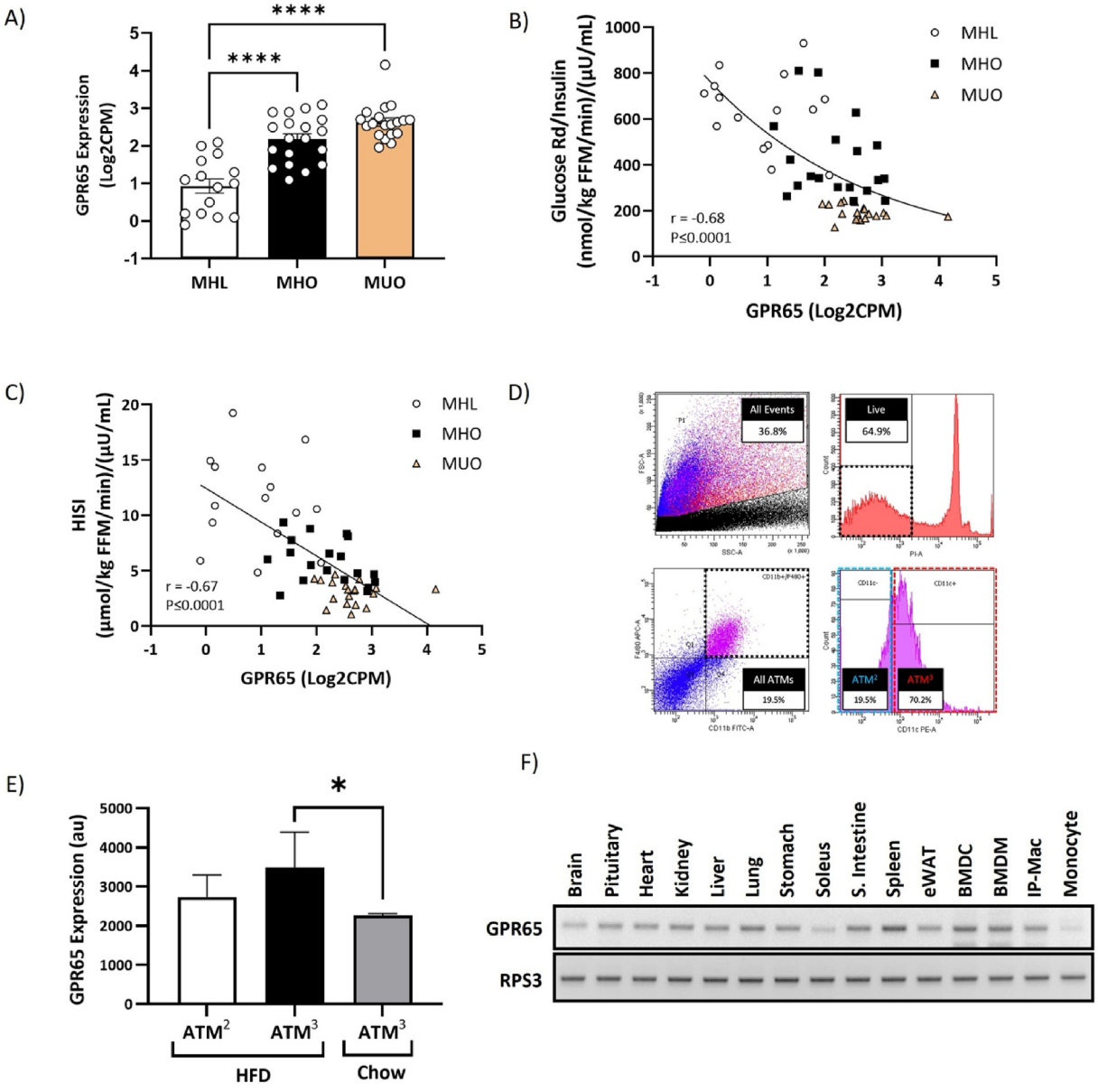

Figure 1: GPR65 expression is elevated in the adipose tissue of individuals with obesity and in the adipose tissue pro-inflammatory macrophage population of HFD-fed mice: A: Subcutaneous abdominal adipose tissue *GPR65* expression in metabolically healthy lean (MHL; $n = 15$), metabolically healthy obese (MHO; $n = 19$), and metabolically unhealthy obese (MUO; $n = 19$) groups. **B—C:** Relationship between adipose tissue *GPR65* expression and skeletal muscle insulin sensitivity (glucose rate of disappearance expressed per kg fat-free mass [FFM] relative to plasma insulin concentration during the hyperinsulinemic-euglycemic clamp procedure [glucose Rd/Insulin]) and the hepatic insulin sensitivity index (HISI, reciprocal of the product of endogenous glucose production rate/kg FFM and plasma insulin concentration during basal conditions). **D-E:** Mice were fed either a chow or high-fat diet (HFD) for 16 weeks, then their adipose tissue macrophages (ATM) isolated and characterized. **(D)** Isolation and gating of FACS sorted ATM, **(E)** ATM GPR65 expression across populations double positive (ATM^2) or triple positive (ATM^3) for macrophage markers ($n = 8—9$/group). **(F)** *GPR65* expression across tissues in a chow-fed mouse. Data are presented as means ± SEM. ($^*P < 0.05$, $^{****}P < 0.0001$). eWAT, epididymal white adipose tissue; S. intestine, small intestine; BMDC, bone marrow derived dendritic cells; BMDM, bone marrow derived macrophages; IP-mac, intraperitoneal macrophages.

humans, AT *GPR65* expression is inversely associated with obesity and positively associated with insulin resistance.

As shown above, *GPR65* is expressed in human adipose tissue [35], however studies have demonstrated expression in immune cells [36]. Thus, the elevations in AT *GPR65* mRNA levels observed here are likely due to either upregulated *GPR65* expression in the resident AT immune cells or an increase in immune cell infiltration. This is consistent with data from others showing that pro-inflammatory macrophage infiltration and subsequent cytokine release is key in the development of AT dysfunction and pathogenesis of insulin resistance [4]. To further interrogate the relationship between the adipose—immune axis and *GPR65* expression, we isolated the immune cell-containing stromal vascular fraction (SVF) from the AT of mice fed a 60% high-fat diet (HFD) for 16 weeks and FACS sorted them based on AT macrophage (ATM) marker expression (Figure 1D). Additionally, a cohort of HFD-fed mice for 16 weeks was switched to a chow diet to determine if the increase in *GPR65* expression upon HFD feeding could be reversed by dietary intervention. *GPR65* expression was elevated in the ATM

population that were triple positive for the pro-inflammatory markers F4/80, CD11b and CD11c (ATM^3), compared to ATMs that were positive for F4/80 and CD11b alone (ATM^2) ($P < 0.05$; Figure 1E); suggesting *GPR65* expression increases with pro-inflammatory polarization. Consistent with this observation, *GPR65* expression decreased in the population of ATM^3 isolated from HFD-fed mice reverted back to a chow diet ($P < 0.05$; Figure 1E), confirming that *GPR65* expression is positively correlated with proinflammatory tone, and the number of ATMs in mice. In contrast to data in humans, *GPR65* expression was detected in several murine tissues, including insulin responsive tissues such as liver, skeletal muscle, and white AT (WAT) (Figure 1F) suggesting that GPR65 may play a role in modulating insulin sensitivity beyond the adipose tissue.

3.2. GPR65 knockout mice display improved insulin sensitivity

Since our initial observation of the elevated *GPR65* expression in proinflammatory ATMs after HFD feeding supported a possible metabolic regulatory role for GPR65, we investigated the role of GPR65 on more holistic indices of metabolic health. We generated a whole-body GPR65 KO mouse line and measured differences in fasting insulin and glucose levels between KO and WT littermates fed an HFD. There were no differences in body weight in WT and KO animals (data not shown). Both fasting glucose and insulin were significantly decreased in GPR65 KO animals compared to WT ($P < 0.05$; Figure 2A,B), indicating a possible insulin sensitizing effect of GPR65 depletion. In line with this, GPR65 KO mice showed significant improvements in blood glucose levels during an oral glucose tolerance test (OGTT) compared with WT littermates, both throughout the experimental time course and in the AUC ($P < 0.05$; Figure 2C,D).

To further assess whole-body insulin sensitivity and to delineate the tissues responsible for improved glucose tolerance in GPR65 KO mice, we performed a hyperinsulinemic-euglycemic clamp. GPR65 KO mice required a glucose infusion rate (GIR) nearly twice that of WT littermates to maintain euglycemia ($P < 0.05$; Figure 2E). Suppression of hepatic glucose production (HGP) during clamp was also significantly improved in GPR65 KO animals compared with WT littermates ($P < 0.05$; Figure 2H). Although total glucose disposal rate (GDR) remained similar between groups (Figure 2F), insulin-stimulated GDR (IS-GDR) at clamp, which reflects muscle insulin sensitivity, was significantly increased in GPR65 KO animals compared with WT littermates ($P < 0.05$; Figure 2G), together suggesting an improvement in whole-body insulin sensitivity after GPR65 deletion.

3.3. Increased mitochondrial activity and fatty acid oxidation in GPR65 KO animals contribute to improved insulin sensitization in the liver

To investigate why GPR65 depletion suppresses HGP and improves hepatic insulin sensitivity, we characterized the hepatic phenotype of these mice. A significant driver of hepatic insulin resistance in HFD-induced obesity is the anomalous accumulation of triglycerides (TG), leading to hepatic steatosis [37]. Lipotoxicity from intracellular lipid intermediates such as diacylglycerols (DAG) and ceramides are correlated with impaired insulin sensitivity and have been shown to interfere with the insulin receptor signaling pathways [38].

Indeed, Oil Red O (ORO) staining of neutral lipids in liver sections from GPR65 KO and WT animals revealed decreased lipid accumulation in KO animals compared with WT littermates (Figure 3A). Consistent with ORO staining, liver TG content measured biochemically, was significantly decreased in KO animals compared to WT littermates ($P < 0.05$; Figure 3B).

Previous studies have demonstrated mitochondrial dysfunction such as primary oxidative phosphorylation (OxPhos) deficiency contributes to hepatic insulin resistance [39]. We asked whether markers of OxPhos are elevated in our GPR65 KO mouse line. Expression of mitochondrial genes involved in mitochondrial maintenance and biogenesis such as transcription factor A mitochondrial (TFAM), the dUTPase isoform Ndut, nuclear respiratory factor (NRF), and key genes regulating thermogenesis, such as uncoupling protein (UCP)1 and UCP3 are increased in the livers of GPR65 KO mice ($P < 0.05$; Figure 3C). Additionally, there was a significant increase of mitochondrial Complex I and Complex IV activity in the livers of GPR65 KO animals, compared to WT littermates ($P < 0.05$; Figure 3D), suggesting enhanced mitochondrial oxidative phosphorylation. Consistent with our observation of decreased liver TG content and enhanced Complex I and IV expression in GPR65 KO mice, β-oxidation of fatty acids was significantly increased in the livers of GPR65 KO mice ($P < 0.05$; Figure 3E). Moreover, the ratio of NADH to NAD^+ and concentration of ATP were similarly elevated in GPR65-KO livers ($P < 0.05$; Figure 3F,G), supporting an elevated rate of oxidative phosphorylation. These data demonstrate GPR65 deficiency improves mitochondrial function, and confers at least in part, improved hepatic insulin sensitivity.

To further investigate the whole-body insulin sensitizing effect of GPR65 KO, we then performed an acute insulin response study in the skeletal muscle; wherein, insulin was injected through the inferior vena cava of fasted and anesthetized mice, and muscle excised for analysis both under basal conditions and 5 min post insulin injection. Upon stimulation with insulin, phosphorylation of Akt at Ser473 was markedly increased in the skeletal muscle of GPR65 KO animals, compared to WT littermates ($P < 0.05$; Figure 3H,I). Together, these data suggest that GPR65 depletion confers improvements in insulin sensitivity in both the liver and skeletal muscle.

3.4. GPR65 KO animals have improved adipose tissue and serum cytokine profiles, resulting in decreased chemotaxis, inflammation and increased M2 polarization

Since we initially observed elevated *GPR65* expression in the AT of people with obesity, and macrophage infiltration in obese AT is a hallmark of insulin resistance, we next examined whether GPR65 deficiency alters AT inflammatory tone and cytokine release. In GPR65 KO mice circulating cytokines such as tumor necrosis factor (TNF)α, macrophage inflammatory protein (MIP)-1β, IL-6, IL-12 p40, and chemokine c–c motif ligand (CCL)5 were markedly reduced ($P < 0.05$; Figure 4A), whereas, anti-inflammatory IL-10 levels showed a non-significant increase ($P > 0.05$; Figure 4A). We observed a significant down regulation of genes associated with pro-inflammatory "M1" macrophages such as keratinocyte-derived cytokine (KC), and cluster of differentiation (CD)80 and CD86 in the AT of GPR65 KO mice ($P < 0.05$; Figure 4B). On the other hand, anti-inflammatory or "M2" markers such as Arginase (Arg), interleukin (IL)-10, and macrophage galactose-type lectin (MGL)1 were upregulated in the AT of GPR65 KO mice ($P < 0.05$; Figure 4C). Overall, these results indicate that GPR65 deficiency leads to an anti-inflammatory phenotype in HFD-fed mice.

Since GPR65 expression is known to be enriched in immune cells, we then sought to determine the effects of GPR65 deletion in macrophages. To this end, we utilized an *in vitro* transwell chemotaxis assay to measure the migratory capacity of intraperitoneal macrophages (IP-Macs) derived from WT or GPR65 KO mice towards adipocytes. Macrophages harvested from WT mice migrated robustly towards the conditioned media (CM) harvested from 3T3-L1 adipocytes, whereas

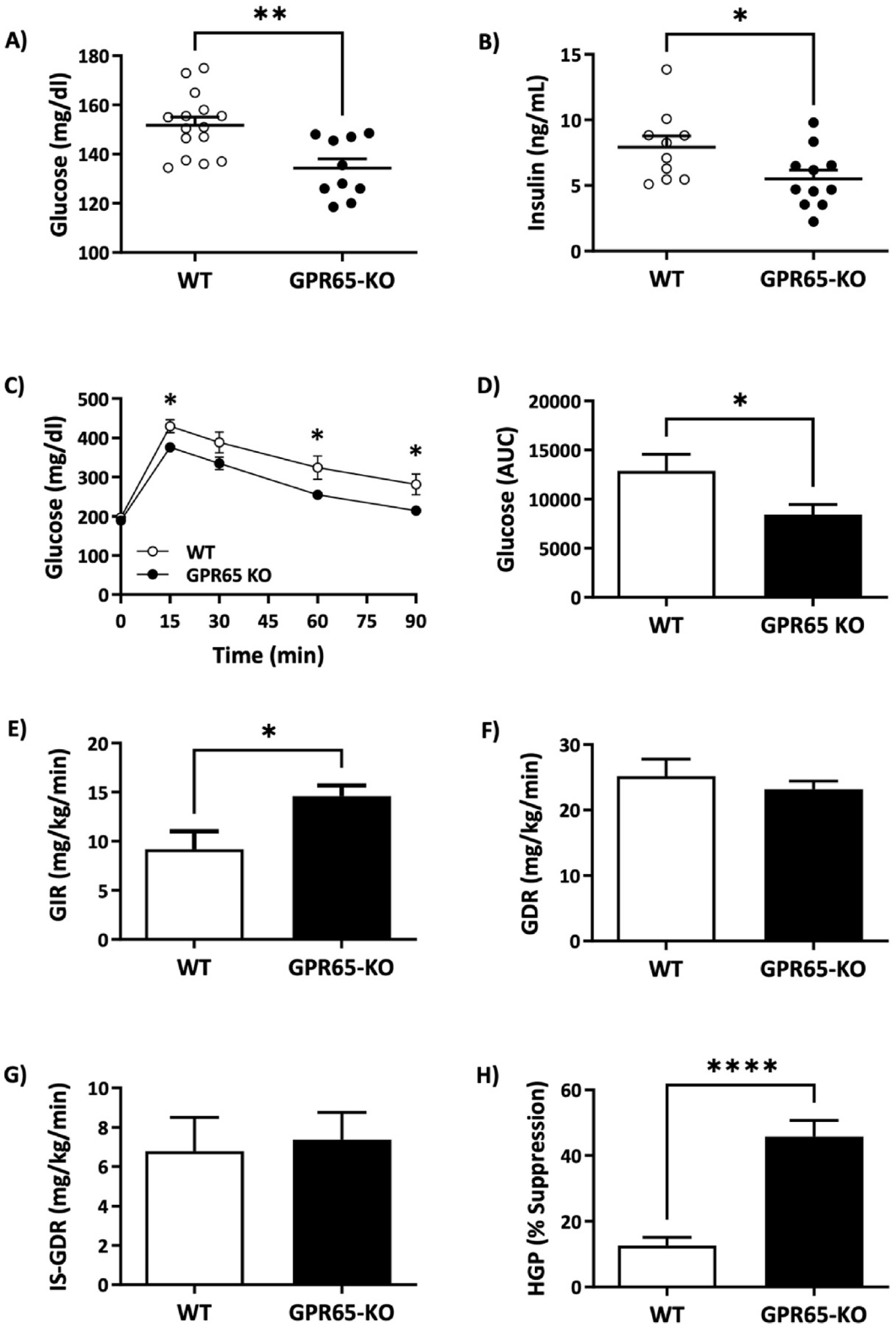

Figure 2: GPR65 mice have improved insulin sensitivity. Whole-body GPR65 knockout (KO) mice or wildtype (WT) littermates were fed on a high-fat diet for 16 weeks before undergoing an oral glucose tolerance test (OGTT) **(C**—**D)** or a hyperinsulinemic-euglycemic clamp **(E**—**H)**. **(A)** fasting blood glucose, **(B)** fasting plasma insulin, **(C)** OGTT, **(D)** OGTT AUC, **(E)** glucose infusion rate, **(F)** glucose disposal rate, **(G)** insulin-stimulated glucose disposal rate, **(H)** suppression of hepatic glucose production. Data is presented as means ± SEM ($n = 10$—15/group) (*$P < 0.05$). AUC, area under the curve; GIR, glucose infusion rate; GDR, glucose disposal rate; IS-GDR, insulin-stimulated GDR; HGP, hepatic glucose production.

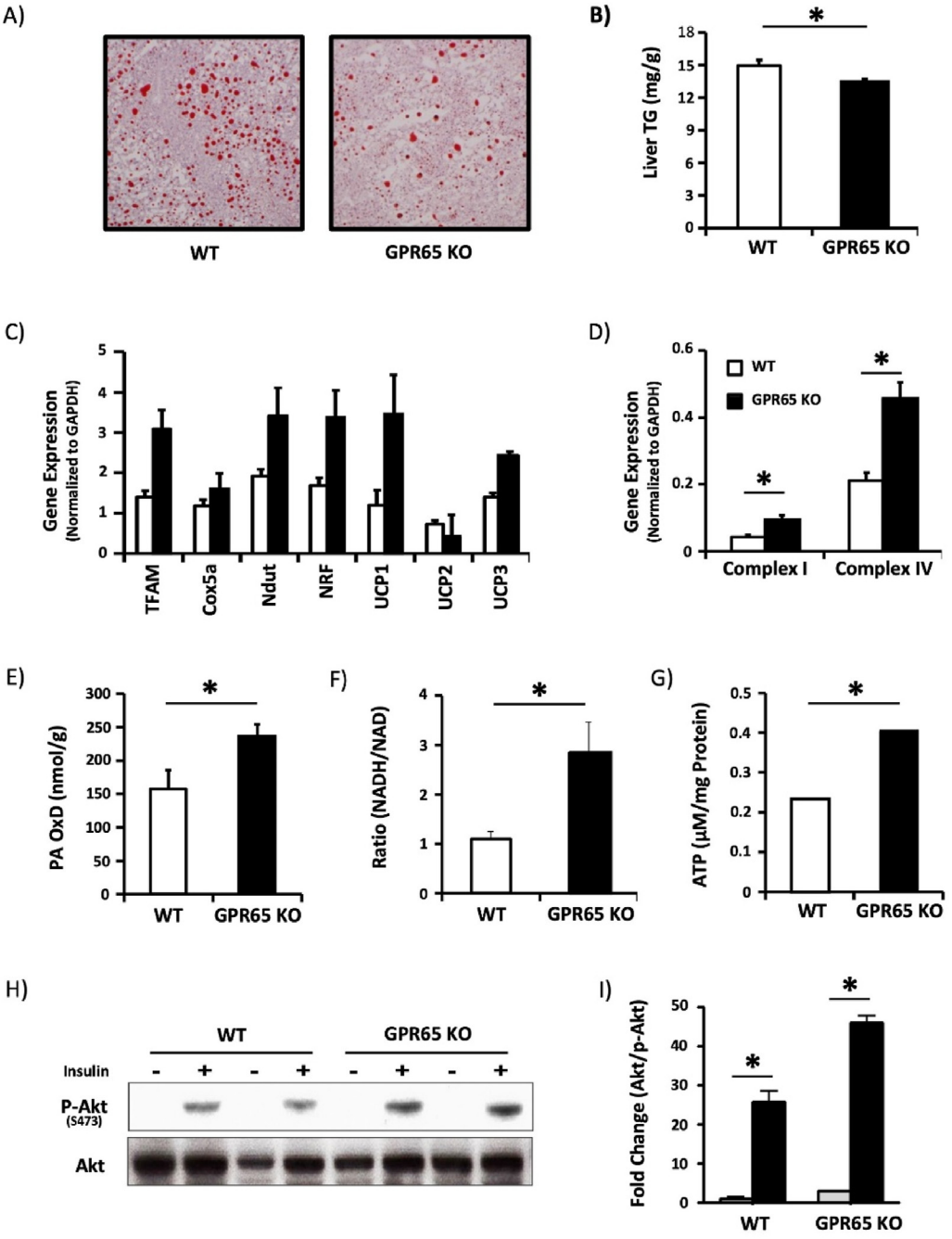

Figure 3: Increased mitochondrial activity and fatty acid oxidation in GPR65 KO mice contribute to improved insulin sensitization in the liver and skeletal muscle. A-G: Comparison of key metabolic marker in the livers of GPR65 KO mice or WT littermates. **(A)** Representative Oil Red O staining, **(B)** liver TG, **(C)** thermogenic gene expression, **(D)** mitochondrial complex gene expression, **(E)** palmitic acid oxidation, **(F)** ratio of NADH to NAD, **(G)** ATP concentration. **H—I:** Acute insulin response study in skeletal muscle. **(H)** Representative blots of phosphorylated-Akt$^{(S473)}$ and Akt, **(I)** quantification of relative change in Akt/p-Akt ratio. Data is presented as means ± SEM ($n = 8-9$/group) ($^*P < 0.05$). TG, triglyceride; TFAM, transcription factor A mitochondrial; Cox5a, cytochrome C oxidase subunit 5a; Ndut, dUTPase; NRF, nuclear respiratory factor; UCP, uncoupling protein; PA OxD, palmitic acid oxidation; NAD, nicotinamide adenine dinucleotide. (For interpretation of the references to color in this figure legend, the reader is referred to the Web version of this article.)

macrophages harvested from GPR65 KO animals showed a dramatic decrease in migratory activity ($P < 0.05$; Figure 4D).

To confirm this finding in a cell autonomous way, we obtained pluripotent hematopoietic stem cells (HSCs) from bone marrow of WT and GPR65 KO mice, differentiated them into bone marrow derived dendritic cells (BMDCs), and then challenged them with lipopolysaccharide (LPS). As expected, LPS treatment caused a dose-dependent increase in the phosphorylation of proinflammatory signaling pathways, including the central regulator of nuclear factor (NF)-κB expression, IκB kinase (IKK), and a major pro-inflammatory signaling cassette mitogen-activated protein kinase (MAPK), c-Jun N-terminal kinase (JNK) ($P < 0.05$; Figure 4E). However, in GPR65-

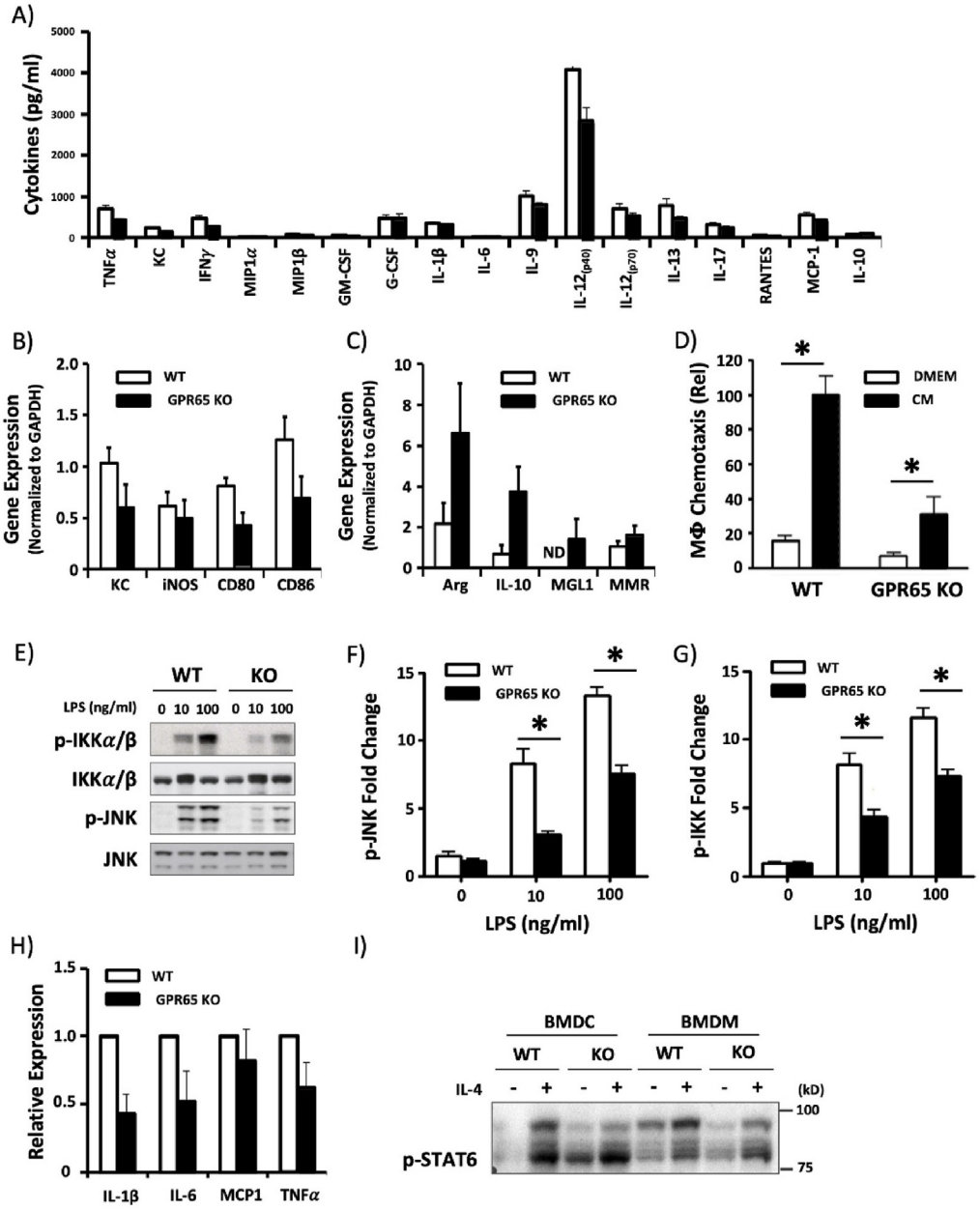

Figure 4: GPR65 deletion reduces systemic inflammation, blunts monocyte infiltration, and increases M2 macrophage polarization. **A-C:** GPR65 KO mice or WT littermates were fed HFD for 16 weeks, then anesthetized and tissues and whole blood isolated. A) Serum cytokines, **B)** adipose tissue proinflammatory "M1" gene expression, **C)** adipose tissue anti-inflammatory "M2" gene expression. **D:** Intraperitoneal macrophages were isolated and seeded into a transwell co-culture system, then conditioned media (CM) from 3T3-L1 adipocytes placed in the adjacent transwell to determine chemotaxis. **D)** Macrophage chemotaxis assay. **E-I:** Pluripotent hematopoietic stem cells were obtained from the bone marrow (BM) of GPR65 KO mice or WT littermates and differentiated into either BM-derived dendritic cells (BMDC) or BM-derived macrophages (BMDM), then challenged with lipopolysaccharide (LPS). **E)** Representative blots of inflammatory signaling pathways, **F)** quantification of p-JNK fold change, **G)** quantification of p-IKK fold change. A Subset of BMDM were also treated with anti-inflammatory IL-4 to see amenability to M2 polarization. **H)** Relative gene expression of BMDM, **I)** representative blot of p-STAT6 in cells treated with/without IL-4. Data is presented as means ± SEM ($n = 8-9$/group) ($^*P < 0.05$). TNFα, tumor necrosis factor α; KC, keratinocyte-derived cytokine (CXCL1); IFNg, interferon-g; MIP1a, macrophage inflammatory protein-1a; MIP3a, macrophage inflammatory protein-3a; GM-CSF, granulocyte-macrophage colony-stimulating factor; G-CSF, granulocyte colony-stimulating factor; IL, interleukin; RANTES, regulated upon activation normal T-cell expressed and secreted; MCP-1, macrophage chemoattractant protein-1.

deficient BMDCs, activation of these pathways by LPS was significantly diminished ($P < 0.05$; Figure 4E—G). Gene expression analysis of BMDCs from GPR65 KO mice revealed that the relative abundance of IL-1β, IL-6 and TNFα is significantly decreased compared to cells from WT mice ($P < 0.05$; Figure 4H). These observations are consistent with decreased serum cytokine levels seen in GPR65 KO animals relative to WT littermates (Figure 4A).

The anti-inflammatory phenotype seen in GPR65 KO mice may be explained in part by a polarization bias in the macrophage population toward an "M2" like phenotype. To explore this, we treated BMDCs

and bone marrow derived macrophages (BMDM) from WT and GPR65 KO mice with the anti-inflammatory cytokine IL-4, which has been shown to promote an alternative "M2" activation of monocytes. Consistent with earlier findings, IL-4-induced a significantly greater increase in phosphorylation of signal transducer and activator of transcription (STAT)6, a marker of M2 signaling, in GPR65 deficient BMDCs compared to WT ($P < 0.05$; Figure 4I). Moreover, GPR65 KO BDMCs exhibited higher basal phosphorylation of STAT6, suggesting they are primed toward an M2 phenotype ($P < 0.05$; Figure 4I). Surprisingly, while IL-4 was able to induce M2 macrophage polarization in BMDMs in both genotypes, we did not observe a difference in the degree of polarization ($P > 0.05$; Figure 4I). Whether there is specificity in the priming of HSC-derived monocytes or the differences in differentiation protocol between BMDCs and BMDMs overrode any inherent bias remains unclear. Overall, our results support the hypothesis that GPR65 deficiency in immune cells polarizes them towards an anti-inflammatory state.

3.5. GPR65 deletion in hematopoietic cells causes improved insulin sensitivity

Given that GPR65 is primarily expressed in immune cells and the observed anti-inflammatory phenotype of GPR65 deficiency, to confirm that myeloid cells are the primary contributor to improved insulin sensitivity in GPR65 KO animals, we used an adoptive transfer approach to transplant bone marrow from either GPR65 KO or WT donor animals to irradiated WT recipients, thereby creating a hematopoietic lineage-specific GPR65 KO mouse. We saw no difference in insulin sensitivity in recipient chow-fed mice that received a bone marrow transplant (BMT) from either GPR65 KO mice or WT littermates ($P > 0.05$; Supp Fig. 1A–D). However, In line with HFD-fed whole-body GPR65 KO mice, recipient mice with BMT from GPR65-KO mice (GPR65 KO^{BMT}) mice showed improved glucose tolerance compared with those with BMT from wildtype mice (WT^{BMT}) in OGTTs ($P < 0.05$; Figure 5A), as well as significantly lower fasting insulin levels ($P < 0.05$; Figure 4B) after HFD feeding. To further assess whole-body

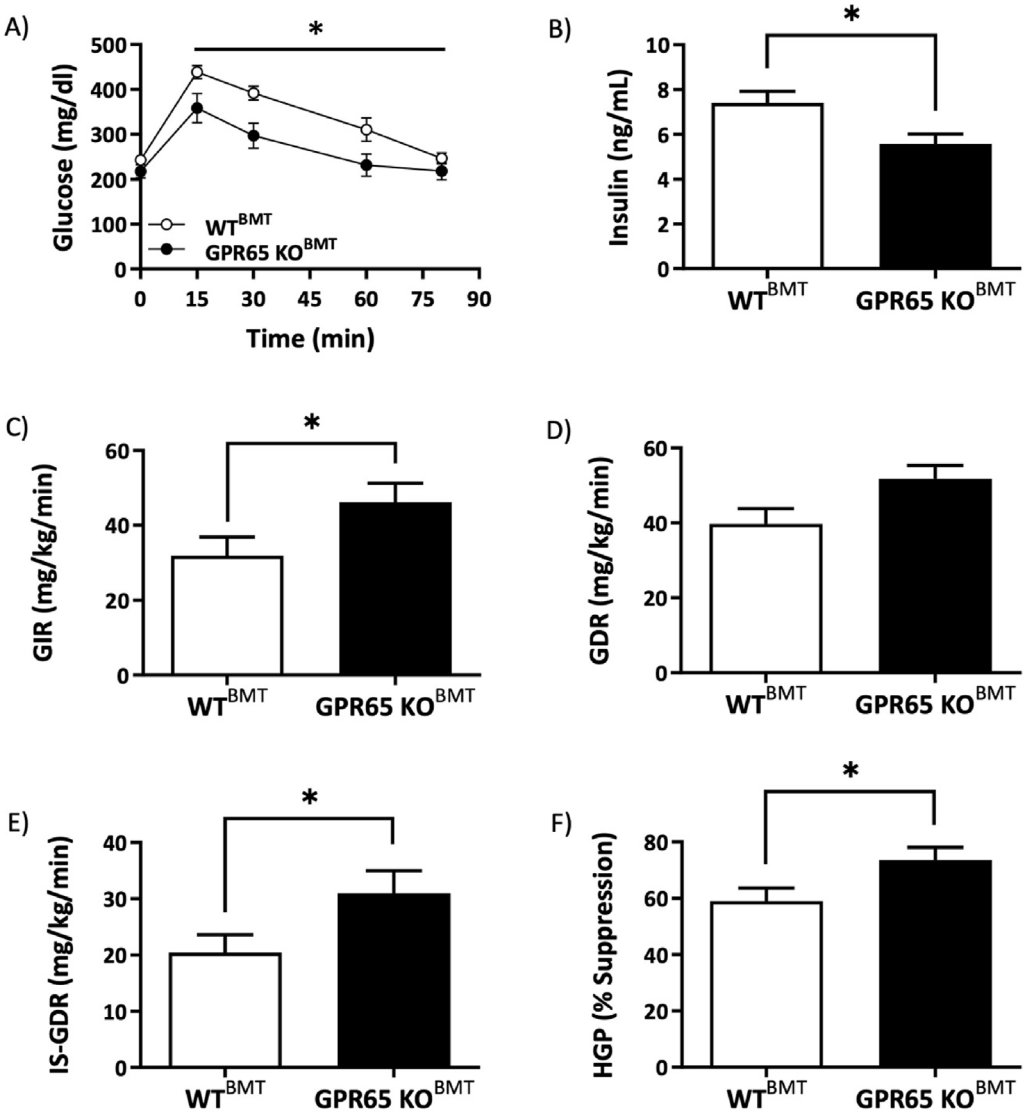

Figure 5: GPR65 deletion in hematopoietic cells improves insulin sensitivity in HFD-fed mice. Bone marrow from GPR65 KO mice or WT littermates was transplanted into WT C57BL/6 mice, creating myeloid-specific GPR65 KO mice. Mice were then fed HFD for 16 weeks. **A)** Oral glucose tolerance test, **B)** fasting insulin. Mice then underwent a hyperinsulinemic-euglycemic clamp. **C)** Glucose infusion rate, **D)** glucose disposal rate, **E)** insulin-stimulated glucose disposal rate, **F)** suppression of hepatic glucose production. Data is presented as means ± SEM ($n = 8–9$/group) (*$P < 0.05$).

insulin sensitivity, we performed hyperinsulinemic-euglycemic clamp studies to evaluate glucose homeostasis in these mice. Consistent with earlier data using global GPR65 KOs, the GIR required to maintain euglycemia was significantly higher in GPR65 KO^{BMT} animals, compared to WT^{BMT} ($P < 0.05$; Figure 5C). Similarly, IS-GDR was elevated and HGP depressed in GPR65 KO^{BMT} mice compared to WT^{BMT}, suggesting enhanced insulin sensitivity in liver and skeletal muscle ($P < 0.05$; Figure 5E,F). These results demonstrate GPR65 deficiency in cells of myeloid lineage confers whole-body insulin sensitivity in mice on an HFD.

4. DISCUSSION

Obesity-associated insulin resistance in metabolic tissues such as fat, liver, and skeletal muscle is now recognized to be the result of a confluence of metabolic dysfunctions. However, among these contributing factors, chronic low-grade chronic inflammation incited by immune cell infiltration — particularly in the adipose tissue, is considered to be a key contributor in the development of whole-body insulin resistance [2—4]. Several members of the innate and adaptive immune system such as neutrophils, T regulatory cells, mast cells, eosinophils, and macrophages have been detected in the adipose tissue and shown to play a role in inflammation and insulin resistance (reviewed elsewhere, [40,41]). Among these immune cell populations, macrophages are the primary effector cells causing metabolic dysfunction [4]. Here, we investigated the role of GPR65, a proton/pH sensor that is primarily expressed in immune cells, in modulating inflammatory responses and multi-tissue insulin sensitivity.

Notably, in human AT, *GPR65* expression was elevated in both metabolically healthy and unhealthy subjects with obesity, and negatively correlated to muscular and hepatic insulin sensitivity, suggesting that GPR65 influences multi-organ insulin sensitivity under states of metabolic distress. GWAS studies have identified the association between *GPR65* variants and a variety of inflammatory diseases such as multiple sclerosis [42], IBD [43—45], ankylosing spondylitis [46] and atopic dermatitis [47]. Indeed, in IBD patients biopsies from inflamed tissues compared to non-inflamed tissues show elevated *GPR65* expression [48] which is likely linked to the degree of macrophage infiltration where GPR65 is highly expressed. Similarly, people suffering from the chronic spinal inflammatory disease ankylosing spondylitis exhibit elevated spinal *GPR65* expression and GPR65-positive cells display elevated levels of IFN-γ and TNFα [49]. *GPR65* expression is also elevated in patients suffering from early pregnancy loss, where GPR65 modulates the activity of extravillous trophoblasts during placental development when the uterine endometrium becomes acidic and hypoxic [50]. More recently, elevated *GPR65* expression has been linked to tumoral size in patients with obesity and is positively correlated with tumoral burden [51]. Elevated *GPR65* expression is seen particularly in gliomas [52], where it is positively correlated to pathological grade and shortened patient survival [53]. This association with cancer is significant, as macrophages often constitute the largest infiltrating immune population in solid tumors [54], and tumoral lactic acid production and acidity is a hallmark of cancer [55]. This also explains the high association between GPR65 and Glioma, where acidity is a common feature [56], and change in intratumoral pH has been proposed as a physiological readout of therapeutic response [57]. Our observation of elevated *GPR65* expression in the AT of patients with obesity is in line with these reports, as excessive AT expansion [58], like aforementioned disease states, is associated with significant macrophage infiltration and immune dysfunction. Importantly, increases in inflammatory tone are directly linked to insulin resistance [59,60], and muscular and hepatic insulin resistance increased with AT *GPR65* expression in our MUO patient cohort. These observations in humans are correlated with the fact that HFD-fed whole-body GPR65 KO mice exhibited enhanced muscular and hepatic insulin sensitivity compared to WT littermates during a hyperinsulinemic-euglycemic clamp. In the liver, this improvement was likely mediated by enhanced mitochondrial oxidative phosphorylation, as evidenced by increased mRNA expression of mitochondrial maintenance and biogenesis genes, thermogenic genes, and Complex I and Complex IV activity. In line with this, we also observed concomitant rises in NADH/NAD^+ ratio and ATP production. These improvements in metabolic capacity also explain the observed increase in palmitic acid oxidation, and the reduction in liver fat content in GPR65 KO animals. Interestingly, GPR65 expression has been shown to influence lipid droplet turnover in other cells via regulation of lysosomal function [61]. How autophagy is impacted in our model may be an interesting area for future investigation. Notably, of any organ, the liver has the largest proportion of its non-parenchymal cell population consisting of immune cells (~20—35%), and resident Kupffer cells are polarized toward an M1 phenotype during obesity [6]. HFD feeding has also been shown to induce a 6-fold increase in monocyte-derived macrophage levels in the livers of obese mice, and hepatic inflammation is directly linked to insulin resistance [6]. Moreover, lipotoxicity and inflammation in the liver are associated with impairments in mitochondrial oxidative phosphorylation [62]. Thus, we propose that the anti-inflammatory effects of GPR65 KO are responsible for the improved hepatic metabolic phenotype in our model.

This is in line with our observation that GPR65 KO suppresses LPS-induced NF-κB, MAPK, and JNK signaling in BMDCs. Recently, hepatic GPR65 signaling has been further associated with metabolic dysfunction, as its expression is elevated in the livers of obese mice and humans with hepatocellular carcinoma, and liver tumor mass was reduced in HFD-fed GPR65 KO mice but not their chow-fed controls [63]. Similarly, others have shown that GPR65 KO suppresses hepatic JNK and NF-κB expression, leading to improvements in inflammation and fibrosis [64].

To our knowledge, we are the first to demonstrate a role for GPR65 in modulating insulin sensitivity in skeletal muscle, wherein, we were able to observe an inverse correlation between AT GPR65 expression and muscular glucose disposal rate in humans. This novel observation that elevated GPR65 expression suppresses muscular insulin sensitivity was recapitulated in our GPR65 KO mouse model, where an acute insulin challenge caused significantly greater phosphorylation of muscular Akt in HFD-fed GPR65 KO mice compared to WT littermates. Consistent with our MHL human cohort where AT GPR65 expression was lowest, these GPR65 KO mice demonstrated markedly higher IS-GDR during hyperinsulinemic-euglycemic clamp, the gold standard for measuring muscular insulin sensitivity. As with the liver, we hypothesize that this improvement is largely driven by reduced inflammatory tone and macrophage infiltration, and is consistent with human single cell RNAseq data, where GPR65 expression in muscle is largely limited to T-cells and macrophages (gene data available from v24.0. www.proteinatlas.org, [65]). In people with obesity, there is elevated intra-muscular adipose tissue (IMAT) which becomes inflamed and infiltrated by immune cells similar to white AT [66]. This infiltration contributes to localized hypoxia, shifting resident myocytes towards anaerobic glycolysis, resulting in lactate buildup in the extracellular space, and acidifying the tissue. Decreased pH itself has been shown to cause impaired insulin receptor phosphorylation [67] and PI3K activity in cultured myoblasts [68], and there is an increased interconversion of pyruvate

to lactate in muscles of T2D individuals [69] making the tissue susceptible to lowered pH.

GPR65 deficiency in our model may reduce immune cell infiltration into muscle, decrease local oxidative demands, and possibly preserve oxidative phosphorylation, which reduces lactate production and ultimately maintains homeostatic extracellular pH. This hypothesis is in line with our observation that GPR65 KO significantly attenuated macrophage chemotaxis towards adipocyte conditioned medium and reduced circulating chemoattractant cytokines such as MIP-1b and CCL5. In addition, GPR65 KO may also prevent pro-inflammatory polarization of resident muscle macrophages during obesity, mitigating extravasation of fluid into the muscle which would impair oxygen diffusion to myocytes and promote glycolysis. Correspondingly, the muscle of obese Zucker rats has been shown to have a 30—50% increase in albumin content due to extravasation [70], and forced expression of GPR65 in macrophages has been associated with "M1" macrophage polarization and TNFα and IL-6 secretion [64]. Conversely, GPR65 KO in our model reduced AT expression of M1 macrophage markers, increased AT expression of M2 macrophage markers, and promoted BMDCs to polarize towards an anti-inflammatory phenotype *in vitro*. Future studies in immunocompromised mice or in MCP-1 KO mice which lack macrophage infiltration into the muscle upon HFD feeding [71] could confirm this hypothesis. However, chow-fed lean mice which received a BMT from GPR65 KO mice or WT littermates showed no variance in insulin sensitivity during hyperinsulinemic-euglycemic clamp. Thus, it is likely that the effects observed here in obese skeletal muscle are driven by intramuscular macrophage accumulation and altered inflammatory tone.

Interestingly, while our data indicates that GPR65 is a pro-inflammatory immune modulator in HFD-induced obesity, there are reports which contradict this finding. Namely, Mogi et al. reported that LPS-induced TNFα secretion was diminished under conditions of extracellular acidification mediated by GPR65 [10]. Similarly, Onozawa et al. observed that pharmacological stimulation of GPR65 with an agonist suppressed LPS-induced TNFα and IL-6 secretion in intraperitoneal macrophages (IP-Macs), while increasing IL-10 secretion [72]. This discordance may be explained by the largely "sterile" and multifactorial nature of the HFD-induced inflammatory microenvironment of our model, whereas inflammation was induced solely via the bacterial byproduct, LPS, in others' experiments. Alternatively, the temporal differences in inflammation may explain the differing results. IP-Macs in other studies were stimulated acutely, whereas inflammatory tone in our experiments is instigated by long-term HFD feeding, which may have desensitized any acute beneficial effects of GPR65. That said, mice expressing the loss-of-function GPR65 variant I231L have defects in Th17 and Th22 differentiation, leading to dysregulated cytokine secretion and an inherent susceptibility to T-cell-driven colitis [73]. However, conditional knockout of GPR65 in $CD4^+$ T-cells ameliorated trinitrobenzene sulfonic acid-induced colitis in mice by reducing infiltration of not only CD4+ T-cells but also neutrophils and macrophages [19]. Thus, the effects of GPR65 signaling are largely context dependent, and may differ between metabolically healthy and unhealthy states. This is in line with our observation that GPR65 expression is upregulated in the AT of humans under states of metabolic distress, and a recent report that GPR65 expression is elevated in the hepatic macrophages of human and mouse fibrotic livers [64]. Together the data suggest that care should be taken to consider not just metabolic milieu but also tissue-specific pleiotropic effects of GPR65 inhibition when considering it as a potential therapeutic.

Reductions in the mRNA expression of the downstream pro-inflammatory genes such as *Il1b*, *Il6*, and *Tnf* in GPR65 KO mice led to reductions in circulating proinflammatory cytokines such as TNFα, IL-6, and IL-12. TNFα alone has been shown to interfere with insulin signaling through TNFR activation and serine phosphorylation of insulin receptor substrate (IRS)-1 [74]. Similarly, IL-6 has been shown to induce the expression of suppressor of cytokine signaling (SOCS)3, which interferes with tyrosine phosphorylation of the insulin receptor and IRS-1 [75]. In line with this reduction in pro-inflammatory tone, BMDCs derived from GPR65 KO mice had significantly greater STAT6 phosphorylation after treatment with the M2-polarizing cytokine IL-4, suggesting that they're primed towards an anti-inflammatory phenotype. Importantly, M2 macrophages have been shown to maintain insulin sensitivity by secreting factors that prevent immune infiltration in tissue and preserve insulin action even during diet-induced obesity [6,76].

Collectively, our data indicates that the primary cause of insulin sensitization in GPR65 KO mice resides in altered immune cell activity. Wherein, GPR65 KO prevents the inflammatory polarization of macrophages in tissues that become metabolically acidified during obesity such as AT, liver, and muscle; thereby preventing the accretion of macrophage-derived inflammatory cytokines that promote insulin resistance. This is substantiated by the fact that HFD-fed WT mice receiving a BMT from GPR56 KO mice exhibited lower fasting circulating insulin and glucose, and significantly reduced blood glucose during OGTT. Moreover, during hyperinsulinemic-euglycemic clamp, $GPR65^{BMT}$ mice required a significantly greater GIR, with a nearly 4-fold reduction in HGP compared to WT^{BMT} mice. This underscores the possible role of GPR65 in dysregulating immune cell function during HFD-induced obesity. Critically, others have also demonstrated that the protective effects of GPR65 KO are mediated by immune cell modulation, as BMT from GPR65 KO mice similarly attenuated CCl_4-induced hepatic inflammation and fibrosis [64].

Currently, there is great interest and ongoing discovery in the field of obesity and cardiometabolic disease. In particular, glucagon-like peptide (GLP)-1 receptor agonism (GLP-1RA) has demonstrated superior efficacy in both improving insulin sensitivity and inducing body weight loss [77]. GPR65 receptor antagonism may provide an orthogonal therapy for a subset of individuals where weight loss alone may not entirely resolve immune-associated metabolic dysfunction. For example, GPR65 receptor antagonism has recently been proposed as a therapeutic for IBD due to its role in directing immune cell differentiation toward pro-inflammatory Th1 and Th17 cells [19]. While GLP-1R agonists have been shown to be safe and tolerable in patients with IBD [78] and lower the risk of colectomy in IBD outcomes they do not reduce the risk of oral steroid use or advanced therapy initiation [79]. Similarly, others have shown no significant improvement in IBD-related hospitalizations in patients on GLP-1RA [80]. Thus, there is still an unmet therapeutic need in this obese subset of patients. That said, it is again important to contextualize GPR65 activation and inhibition, as missense coding variants of GPR65 are associated with IBD development and GPR65 KO in mice impairs bacterial phagocytosis and activates the NLRP3 inflammasome [48]. Thus, while GPR65 monotherapy may have off-target effects, co-treatment with a GLP-1RA may be beneficial as its anti-inflammatory actions have been shown to reduce inflammasome activation [81,82].

GPR65 therapy may also be beneficial in other inflammatory disorders associated with obesity such as osteoarthritis [83,84], metabolic dysfunction-associated steatohepatitis (MASH) [64], and atherosclerotic cardiovascular disease. Atherosclerosis particularly presents a significant health burden which is incompletely addressed by GLP-1RA treatment. Notably, GPR65 expression is elevated in the atherosclerotic plaques of ApoE KO mice, and silencing of GPR65 mitigated the

phenotypic transformation and migration of vascular smooth muscle cells [85]. Therefore, while GPR65 antagonism has demonstrated clear insulin sensitizing effects, its therapeutic potential as an immunomodulatory agent is not limited to glucose normalization.

5. CONCLUSIONS

Together, we here demonstrate that during HFD-induced obesity GPR65 plays a pro-inflammatory role contributing to the development of insulin resistance. We also demonstrate that GPR65 KO improves global insulin sensitivity in an immune-dependent manner, by ameliorating pro-inflammatory signaling, macrophage infiltration, and polarizing immune cells towards an anti-inflammatory "M2" phenotype. These data disclose the therapeutic potential of targeting GPR65 to ameliorate inflammation and insulin resistance in obesity.

CRediT AUTHORSHIP CONTRIBUTION STATEMENT

Yingjiang Zhou: Writing — original draft, Validation, Formal analysis, Conceptualization. **EunJu Bae:** Validation, Resources, Methodology, Investigation, Conceptualization. **Simon S. Hoffman:** Writing — original draft, Visualization, Software. **Da Young Oh:** Validation, Methodology, Investigation. **Gordon I. Smith:** Data curation, Formal analysis, Methodology, Writing — review & editing. **Samuel Klein:** Data curation, Formal analysis, Funding acquisition, Investigation, Methodology, Resources, Writing — review & editing. **Saswata Talukdar:** Writing — review & editing, Writing — original draft, Supervision, Funding acquisition, Formal analysis, Data curation, Conceptualization.

DECLARATION OF COMPETING INTEREST

The authors declare the following financial interests/personal relationships which may be considered as potential competing interests: Saswata Talukdar reports financial support was provided by Merck & Co Inc. Saswata Talukdar reports a relationship with Merck & Co Inc that includes: employment and equity or stocks. Yingjiang Zhou reports a relationship with Merck & Co Inc that includes: employment and equity or stocks. Simon Hoffman reports a relationship with Merck & Co Inc that includes: employment and equity or stocks. Saswata Talukdar, Yingjiang Zhou and Simon Hoffman are employees and stockholders of Merck Sharp & Dohme LLC, a subsidiary of Merck & Co., Inc., Rahway, NJ, USA, and/or shareholders of Merck & Co., Inc., Rahway, NJ, USA. No other conflicts exist. If there are other authors, they declare that they have no known competing financial interests or personal relationships that could have appeared to influence the work reported in this paper.

FINANCIAL SUPPORT AND SPONSORSHIP

Clinical data was supported by NIH grants P30 DK056341 (Washington University Nutrition Obesity Research Center) and UL1 TR000448 (Washington University Institute of Clinical and Translational Sciences) awarded to Dr. Samuel Klein. All other work in the manuscript was funded by Merck Sharp & Dohme LLC, a subsidiary of Merck & Co., Inc., Rahway, NJ USA.

DATA AVAILABILITY

Data will be made available on request.

APPENDIX A. SUPPLEMENTARY DATA

Supplementary data to this article can be found online at https://doi.org/10.1016/j.molmet.2025.102169.

REFERENCES

[1] Castro AV, Kolka CM, Kim SP, Bergman RN. Obesity, insulin resistance and comorbidities? Mechanisms of association. Arq Bras Endocrinol Metabol 2014;58(6):600—9.
[2] Gregor MF, Hotamisligil GS. Inflammatory mechanisms in obesity. Annu Rev Immunol 2011;29:415—45.
[3] Donath MY, Shoelson SE. Type 2 diabetes as an inflammatory disease. Nat Rev Immunol 2011;11(2):98—107.
[4] Olefsky JM, Glass CK. Macrophages, inflammation, and insulin resistance. Annu Rev Physiol 2010;72:219—46.
[5] Lindhorst A, Raulien N, Wieghofer P, Eilers J, Rossi FMV, Bechmann I, et al. Adipocyte death triggers a pro-inflammatory response and induces metabolic activation of resident macrophages. Cell Death Dis 2021;12(6):579.
[6] Li H, Meng Y, He S, Tan X, Zhang Y, Zhang X, et al. Macrophages, chronic inflammation, and insulin resistance. Cells 2022;11(19):3001.
[7] Püschel GP, Klauder J, Henkel J. Macrophages, low-grade inflammation, insulin resistance and hyperinsulinemia: A mutual ambiguous relationship in the development of metabolic diseases. J Clin Med 2022;11(15):4358.
[8] Frassetto LA, Masharani U. Effects of alterations in acid—base effects on insulin signaling. Int J Mol Sci 2024;25(5):2739.
[9] Vermeulen ME, Gamberale R, Trevani AS, Martinez D, Ceballos A, Sabatte J, et al. The impact of extracellular acidosis on dendritic cell function. Crit Rev Immunol 2004;24(5):363—84.
[10] Mogi C, Tobo M, Tomura H, Murata N, He XD, Sato K, et al. Involvement of proton-sensing TDAG8 in extracellular acidification-induced inhibition of proinflammatory cytokine production in peritoneal macrophages. J Immunol 2009;182(5):3243—51.
[11] Lardner A. The effects of extracellular pH on immune function. J Leukoc Biol 2001;69(4):522—30.
[12] Imenez Silva PH, Camara NO, Wagner CA. Role of proton-activated G protein-coupled receptors in pathophysiology. Am J Physiol Cell Physiol 2022;323(2):C400—14.
[13] Feng T, Zhao X, Gu P, Yang W, Wang C, Guo Q, et al. Adipocyte-derived lactate is a signalling metabolite that potentiates adipose macrophage inflammation via targeting PHD2. Nat Commun 2022;13(1):5208.
[14] Lambert DC, Abramowitz MK. Obesity, anion accumulation, and anion gap metabolic acidosis: A cohort study. Kidney 2021;360 2(11):1706—15.
[15] Defronzo RA, Beckles AD. Glucose intolerance following chronic metabolic acidosis in man. Am J Physiol Endocrinol Metabol 1979;236(4):E328.
[16] Imenez Silva PH, Wagner CA. Physiological relevance of proton-activated GPCRs. Pflugers Arch 2022;474(5):487—504.
[17] Wang JQ, Kon J, Mogi C, Tobo M, Damirin A, Sato K, et al. TDAG8 is a proton-sensing and psychosine-sensitive G-protein-coupled receptor. J Biol Chem 2004;279(44):45626—33.
[18] Ihara Y, Kihara Y, Hamano F, Yanagida K, Morishita Y, Kunita A, et al. The G protein-coupled receptor T-cell death-associated gene 8 (TDAG8) facilitates tumor development by serving as an extracellular pH sensor. Proc Natl Acad Sci U S A 2010;107(40):17309—14.
[19] Lin R, Wu W, Chen H, Gao H, Wu X, Li G, et al. GPR65 promotes intestinal mucosal Th1 and Th17 cell differentiation and gut inflammation through downregulating NUAK2. Clin Transl Med 2022;12(3):e771.
[20] Erika Rui, David Benjamin, Bradford Stephen. Sensory neurons that detect stretch and nutrients in the digestive system. Cell 2016;166(1):209—21.

[21] Borgmann D, Ciglieri E, Biglari N, Brandt C, Cremer AL, Backes H, et al. Gut-brain communication by distinct sensory neurons differently controls feeding and glucose metabolism. Cell Metabol 2021;33(7):1466–1482.e1467.
[22] Petersen MC, Smith GI, Palacios HH, Farabi SS, Yoshino M, Yoshino J, et al. Cardiometabolic characteristics of people with metabolically healthy and unhealthy obesity. Cell Metabol 2024;36(4):745–761.e745.
[23] Koh H-CE, Van Vliet S, Meyer GA, Laforest R, Gropler RJ, Klein S, et al. Heterogeneity in insulin-stimulated glucose uptake among different muscle groups in healthy lean people and people with obesity. Diabetologia 2021;64(5):1158–68.
[24] Korenblat KM, Fabbrini E, Mohammed BS, Klein S. Liver, muscle, and adipose tissue insulin action is directly related to intrahepatic triglyceride content in obese subjects. Gastroenterology 2008;134(5):1369–75.
[25] Li P, Lu M, Nguyen MTA, Bae EJ, Chapman J, Feng D, et al. Functional heterogeneity of CD11c-positive adipose tissue macrophages in diet-induced obese mice. J Biol Chem 2010;285(20):15333–45.
[26] Osborn O, Oh DY, McNelis J, Sanchez-Alavez M, Talukdar S, Lu M, et al. G protein–coupled receptor 21 deletion improves insulin sensitivity in diet-induced obese mice. J Clin Investig 2012;122(7):2444–53.
[27] Steele R. Influences of glucose loading and of injected insulin on hepatic glucose output. Ann N Y Acad Sci 1959;82(2):420–30.
[28] Hevener AL, He W, Barak Y, Le J, Bandyopadhyay G, Olson P, et al. Muscle-specific Pparg deletion causes insulin resistance. Nat Med 2003;9(12):1491–7.
[29] Nguyen MTA, Satoh H, Favelyukis S, Babendure JL, Imamura T, Sbodio JI, et al. JNK and tumor necrosis factor-α mediate free fatty acid-induced insulin resistance in 3T3-L1 adipocytes. J Biol Chem 2005;280(42):35361–71.
[30] Jun Andrei, Talukdar S, Eek Hae, Park H-W, et al. Maintenance of metabolic homeostasis by Sestrin2 and Sestrin3. Cell Metabol 2012;16(3):311–21.
[31] Koves TR, Noland RC, Bates AL, Henes ST, Muoio DM, Cortright RN. Subsarcolemmal and intermyofibrillar mitochondria play distinct roles in regulating skeletal muscle fatty acid metabolism. Am J Physiol Cell Physiol 2005;288(5):C1074–82.
[32] Glatz JFC, Jacobs AEM, Veerkamp JH. Fatty acid oxidation in human and rat heart. Comparison of cell-free and cellular systems. Biochim Biophys Acta Lipids Lipid Metabol 1984;794(3):454–65.
[33] Nguyen MTA, Favelyukis S, Nguyen A-K, Reichart D, Scott PA, Jenn A, et al. A Subpopulation of macrophages infiltrates hypertrophic adipose tissue and is activated by free fatty acids via toll-like receptors 2 and 4 and JNK-dependent pathways. J Biol Chem 2007;282(48):35279–92.
[34] Patsouris D, Neels JG, Fan W, Li P-P, Nguyen MTA, Olefsky JM. Glucocorticoids and thiazolidinediones interfere with adipocyte-mediated macrophage chemotaxis and recruitment. J Biol Chem 2009;284(45):31223–35.
[35] Amisten S, Neville M, Hawkes R, Persaud SJ, Karpe F, Salehi A. An atlas of G-protein coupled receptor expression and function in human subcutaneous adipose tissue. Pharmacol Ther 2015;146:61–93.
[36] Lattin JE, Schroder K, Su AI, Walker JR, Zhang J, Wiltshire T, et al. Expression analysis of G Protein-Coupled Receptors in mouse macrophages. Immunome Res 2008;4:5.
[37] Borén J, Taskinen MR, Olofsson SO, Levin M. Ectopic lipid storage and insulin resistance: a harmful relationship. J Int Med 2013;274(1):25–40.
[38] Petersen MC, Shulman GI. Roles of diacylglycerols and ceramides in hepatic insulin resistance. Trends Pharmacol Sci 2017;38(7):649–65.
[39] Martin SD, Morrison S, Konstantopoulos N, McGee SL. Mitochondrial dysfunction has divergent, cell type-dependent effects on insulin action. Mol Metabol 2014;3(4):408–18.
[40] Gliniak CM, Pedersen L, Scherer PE. Adipose tissue fibrosis: the unwanted houseguest invited by obesity. Journal of Endocrinology 2023;259(3).
[41] Lee YS, Wollam J, Olefsky JM. An integrated view of immunometabolism. Cell 2018;172(1-2):22–40.
[42] Timasheva Y, Nasibullin TR, Tuktarova IA, Erdman VV, Galiullin TR, Zaplakhova OV, et al. Multilocus evaluation of genetic predictors of multiple sclerosis. Gene 2022;809:146008.
[43] De Lange KM, Moutsianas L, Lee JC, Lamb CA, Luo Y, Kennedy NA, et al. Genome-wide association study implicates immune activation of multiple integrin genes in inflammatory bowel disease. Nat Genet 2017;49(2):256–61.
[44] Jostins L, Ripke S, Weersma RK, Duerr RH, McGovern DP, Hui KY, et al. Host–microbe interactions have shaped the genetic architecture of inflammatory bowel disease. Nature 2012;491(7422):119–24.
[45] Liu JZ, Van Sommeren S, Huang H, Ng SC, Alberts R, Takahashi A, et al. Association analyses identify 38 susceptibility loci for inflammatory bowel disease and highlight shared genetic risk across populations. Nat Genet 2015;47(9):979–86.
[46] Yuan Y, Ma Y, Zhang X, Han R, Hu X, Yang J, et al. Genetic polymorphisms of G protein-coupled receptor 65 gene are associated with ankylosing spondylitis in a Chinese Han population: A case-control study. Hum Immunol 2019;80(2):146–50.
[47] Xie L, McKenzie CI, Qu X, Mu Y, Wang Q, Bing N, et al. pH and proton sensor GPR65 determine susceptibility to atopic dermatitis. J Immunol 2021;207(1):101–9.
[48] Mercier V, Boucher G, Devost D, Bourque K, Alikashani A, Beauchamp C, et al. IBD-associated G protein-coupled receptor 65 variant compromises signalling and impairs key functions involved in inflammation. Cell Signal 2022;93:110294.
[49] Park Y,PK, Jo S, Kim T, Kim T. Enhanced expression of GPR65 in inflammatory sites and bone formation regions in ankylosing spondylitis: evidence from ScRNA-seq analysis [abstract]. Arthritis Rheumatol 2024;(suppl 9).
[50] Mao J, Feng Y, Zheng Y, Gao Y, Zhang L, Sun X, et al. GPR65 inhibits human trophoblast cell adhesion through upregulation of MYLK and downregulation of fibronectin via cAMP-ERK signaling in a low pH environment. Cell Commun Signal 2023;21(1).
[51] Wang L, Sun L, Sun H, Xing Y, Zhou S, An G, et al. GPR65 as a potential immune checkpoint regulates the immune microenvironment according to pan-cancer analysis. Heliyon 2023;9(2):e13617.
[52] Fan J, Liu J, Zhang B, Wang X, Wang X, Liang J, et al. GPR65 contributes to constructing immunosuppressive microenvironment in glioma. Neurosurgical Review 2024;47(1).
[53] Wang H-X, Chen Y-H, Zhou J-X, Hu X-Y, Tan C, Yan Y, et al. Overexpression of G-protein-coupled receptors 65 in glioblastoma predicts poor patient prognosis. Clinical Neurology and Neurosurgery 2018;164:132–7.
[54] Qian B-Z, Pollard JW. Macrophage diversity enhances tumor progression and metastasis. Cell 2010;141(1):39–51.
[55] Bogdanov A, Bogdanov A, Chubenko V, Volkov N, Moiseenko F, Moiseyenko V. Tumor acidity: From hallmark of cancer to target of treatment. Front Oncol 2022;12:979154.
[56] Seyfried TN, Arismendi-Morillo G, Zuccoli G, Lee DC, Duraj T, Elsakka AM, et al. Metabolic management of microenvironment acidity in glioblastoma. Front Oncol 2022;12:968351.
[57] Rao JU, Coman D, Walsh JJ, Ali MM, Huang Y, Hyder F. Temozolomide arrests glioma growth and normalizes intratumoral extracellular pH. Sci Rep 2017;7(1).
[58] Surmi B, Hasty A. Macrophage infiltration into adipose tissue: initiation, propagation and remodeling. Future Lipidol s 2008;3(5):545–56.
[59] Gelaye B, Revilla L, Lopez T, Suarez L, Sanchez SE, Hevner K, et al. Association between insulin resistance and c-reactive protein among Peruvian adults. Diabetol Metab Syndr 2010;2(1):30.
[60] Missel AL, Saslow LR, Griauzde DH, Marvicsin D, Sen A, Richardson CR, et al. Association between fasting insulin and C-reactive protein among adults without diabetes using a two-part model: NHANES 2005-2010. Diabetol Metab Syndr 2021;13(1):29.

[61] Kara Craig, Mari M, Murano T, Begun J, Leigh, et al. Genetic coding variant in GPR65 alters lysosomal pH and links lysosomal dysfunction with colitis risk. Immunity 2016;44(6):1392—405.
[62] Myint M, Oppedisano F, De Giorgi V, Kim B-M, Marincola FM, Alter HJ, et al. Inflammatory signaling in NASH driven by hepatocyte mitochondrial dysfunctions. J Transl Med 2023;21(1).
[63] Bagchi S, Yuan R, Huang H-L, Zhang W, Chiu DK-C, Kim H, et al. The acid-sensing receptor GPR65 on tumor macrophages drives tumor growth in obesity. Sci Immunol 2024;9(100).
[64] Zhang K, Zhang M-X, Meng X-X, Zhu J, Wang J-J, He Y-F, et al. Targeting GPR65 alleviates hepatic inflammation and fibrosis by suppressing the JNK and NF-κB pathways. Milit Med Res 2023;10(1).
[65] Uhlén M, Fagerberg L, Hallström BM, Lindskog C, Oksvold P, Mardinoglu A, et al. Tissue-based map of the human proteome. Science 2015;347(6220). 1260419-1260419.
[66] Wu H, Ballantyne CM. Skeletal muscle inflammation and insulin resistance in obesity. J Clin Investig 2017;127(1):43—54.
[67] Hayata H, Miyazaki H, Niisato N, Yokoyama N, Marunaka Y. Lowered extracellular pH is involved in the pathogenesis of skeletal muscle insulin resistance. Biochem Biophys Res Commun 2014;445(1):170—4.
[68] Franch HA, Raissi S, Wang X, Zheng B, Bailey JL, Price SR. Acidosis impairs insulin receptor substrate-1-associated phosphoinositide 3-kinase signaling in muscle cells: consequences on proteolysis. Am J Physiol Ren Physiol 2004;287(4):F700—6.
[69] Avogaro A, Toffolo G, Miola M, Valerio A, Tiengo A, Cobelli C, et al. Intracellular lactate- and pyruvate-interconversion rates are increased in muscle tissue of non-insulin-dependent diabetic individuals. J Clin Investig 1996;98(1):108—15.
[70] St-Pierre P, Bouffard L, Papirakis ME, Maheux P. Increased extravasation of macromolecules in skeletal muscles of the Zucker rat model. Obesity 2006;14(5):787—93.
[71] Fink LN, Costford SR, Lee YS, Jensen TE, Bilan PJ, Oberbach A, et al. Pro-Inflammatory macrophages increase in skeletal muscle of high fat-Fed mice and correlate with metabolic risk markers in humans. Obesity 2014;22(3):747—57.
[72] Onozawa Y, Fujita Y, Kuwabara H, Nagasaki M, Komai T, Oda T. Activation of T cell death-associated gene 8 regulates the cytokine production of T cells and macrophages in vitro. Eur J Pharmacol 2012;683(1-3):325—31.
[73] Chen X, Jaiswal A, Costliow Z, Herbst P, Creasey EA, Oshiro-Rapley N, et al. pH sensing controls tissue inflammation by modulating cellular metabolism and endo-lysosomal function of immune cells. Nat Immunol 2022;23(7):1063—75.
[74] Peraldi P, Hotamisligil GS, Buurman WA, White MF, Spiegelman BM. Tumor necrosis factor (TNF)-α inhibits insulin signaling through stimulation of the p55 TNF receptor and activation of sphingomyelinase. J Biol Chem 1996;271(22):13018—22.
[75] Rehman K, Akash MSH, Liaqat A, Kamal S, Qadir MI, Rasul A. Role of Interleukin-6 in development of insulin resistance and type 2 diabetes mellitus. Crit Rev Eukaryot Gene Expr 2017;27(3):229—36.
[76] Hong E-G, Ko HJ, Cho Y-R, Kim H-J, Ma Z, Yu TY, et al. Interleukin-10 prevents diet-induced insulin resistance by attenuating macrophage and cytokine response in skeletal muscle. Diabetes 2009;58(11):2525—35.
[77] Resnick O, Bril F, Beauchamp G. Glucagon-like peptide-1 receptor agonists and type 1 diabetes: a potential game changer? Front Endocrinol (Lausanne) 2024;15:1520313.
[78] Desai A, Khataniar H, Hashash JG, Farraye FA, Regueiro M, Kochhar GS. Effectiveness and safety of semaglutide for weight loss in patients with inflammatory bowel disease and obesity. Inflamm Bowel Dis 2025;31(3):696—705.
[79] Desai A, Petrov J, Hashash JG, Patel H, Brahmbhatt B, Kochhar GS, et al. Use of glucagon-like peptide-1 receptor agonists for type 2 diabetes mellitus and outcomes of inflammatory bowel disease. Aliment Pharmacol Ther 2024;60(5):620—32.
[80] Levine I, Sekhri S, Schreiber-Stainthorp W, Locke B, Delau O, Elhawary M, et al. GLP-1 receptor agonists confer no increased rates of IBD exacerbation among patients with IBD. Inflamm Bowel Dis 2025;31(2):467—75.
[81] Chen X, Huang Q, Feng J, Xiao Z, Zhang X, Zhao L. GLP-1 alleviates NLRP3 inflammasome-dependent inflammation in perivascular adipose tissue by inhibiting the NF-κB signalling pathway. J Int Med Res 2021;49(2). 030006052199298.
[82] Wang W, Zhang C, Zhang H, Li L, Fan T, Jin Z. The alleviating effect and mechanism of GLP-1 on ulcerative colitis. Aging 2023;15(16):8044—60.
[83] Meurot C, Jacques C, Martin C, Sudre L, Breton J, Rattenbach R, et al. Targeting the GLP-1/GLP-1R axis to treat osteoarthritis: A new opportunity? J Orthopaed Translat 2022;32:121—9.
[84] Pattison LA, Rickman RH, Hilton H, Dannawi M, Wijesinghe SN, Ladds G, et al. Activation of the proton-sensing GPCR, GPR65 on fibroblast-like synoviocytes contributes to inflammatory joint pain. Proc Natl Acad Sci 2024;121(51).
[85] Chen L-D, Zhu W-T, Cheng Y-Y, Li Z-H, Chen Y-Q, Yuan Z-W, et al. T-cell death-associated gene 8 accelerates atherosclerosis by promoting vascular smooth muscle cell proliferation and migration. Atherosclerosis 2020;297:64—73.

